

## Heat Transfer in MHD Flow of Maxwell Fluid via Fractional Cattaneo-Friedrich Model: A Finite Difference Approach

Muhammad Saqib<sup>1</sup>, Hanifa Hanif<sup>1, 2</sup>, T. Abdeljawad<sup>3, 4, 5</sup>, Ilyas Khan<sup>6, \*</sup>, Sharidan Shafie<sup>1</sup> and Kottakkaran Sooppy Nisar<sup>7</sup>

**Abstract:** The idea of fractional derivatives is applied to several problems of viscoelastic fluid. However, most of these problems (fluid problems), were studied analytically using different integral transform techniques, as most of these problems are linear. The idea of the above fractional derivatives is rarely applied to fluid problems governed by nonlinear partial differential equations. Most importantly, in the nonlinear problems, either the fractional models are developed by artificial replacement of the classical derivatives with fractional derivatives or simple classical problems (without developing the fractional model even using artificial replacement) are solved. These problems were mostly solved for steady-state fluid problems. In the present article, studied unsteady nonlinear non-Newtonian fluid problem (Cattaneo-Friedrich Maxwell (CFM) model) and the fractional model are developed starting from the fractional constitutive equations to the fractional governing equations; in other words, the artificial replacement of the classical derivatives with fractional derivatives is not done, but in details, the fractional problem is modeled from the fractional constitutive equations. More exactly two-dimensional magnetic resistive flow in a porous medium of fractional Maxwell fluid (FMF) over an inclined plate with variable velocity and the temperature is studied. The Caputo time-fractional derivative model (CFM) is used in the governing equations. The proposed model is numerically solved via finite difference method (FDM) along with L1-scheme for discretization. The numerical results are presented in various figures. These results indicated that the fractional parameters significantly affect the temperature and velocity fields. It is noticed that the temperature field increased with an increase in the fractional parameter. Whereas, the effect of fractional parameters is opposite on the velocity field near the plate. However, this trend became like that of the temperature profile, away from

---

<sup>1</sup> Department of Mathematical Sciences, Faculty of Science, Universiti Teknologi Malaysia, Johor Bahru, 81310, Malaysia.

<sup>2</sup> Department of Mathematics, Sardar Bahadur Khan Women's University, Quetta, Pakistan.

<sup>3</sup> Department of Mathematics and General Sciences, Prince Sultan University, Riyadh, 11586, Saudi Arabia.

<sup>4</sup> Department of Medical Research, China Medical University, Taichung, 40402, Taiwan.

<sup>5</sup> Department of Computer Science and Information Engineering, Asia University, Taichung, 40402, Taiwan.

<sup>6</sup> Faculty of Mathematics and Statistics, Ton Duc Thang University, Ho Chi Minh City, Vietnam.

<sup>7</sup> Department of Mathematics, College of Arts and Sciences, Prince Sattam bin Abdulaziz University, Wadi Aldawaser, 11991, Saudi Arabia.

\* Corresponding Author: Ilyas Khan. Email: ilyaskhan@tdtu.edu.vn.

Received: 01 May 2020; Accepted: 05 June 2020.

the plate. Moreover, the velocity field retarded with strengthening in the magnetic parameter due to enhancement in Lorentz force. However, this effect reverses in the case of the temperature profile.

**Keywords:** Viscoelastic fluid, Cattaneo-Friedrich Maxwell model, variable heating, magnetohydrodynamic (MHD), porous medium, fractional derivatives.

## 1 Introduction

In the last 10 decades, it is recognized that fractional calculus can describe hereditary properties and memory effects of materials. It has a wide range of applications in real-world problems which include chaos, diffusion, chemical reaction, dynamics, and viscoelasticity [Khan, Saqib and Ali (2018); Saqib, Shafie, Khan et al. (2020); Sheikh, Ali, Saqib et al. (2017)]. Recently, fractional derivatives are in practice to describe the complicated trends of viscoelastic materials in various physical and industrial areas which include biometric foods, extrusion of polymer fluid, colloidal solutions, cooling of metallic plates, exotic lubricants, glass fiber production, and glass blowing [Haque, Awan, Raza et al. (2018)]. Makris et al. [Makris and Constantinou (1991)] were indicated that it will unconvincing for the Maxwell model with conventional derivatives to obtain enough experimental data because of dissimilar frequencies range. Though Friedrich [Friedrich (1991)] discovered a link between molecular theory and constitutive equations of the Maxwell model with fractional derivatives. Markis et al. [Makris, Dargush and Constantinou (1993)] suggested that an excellent agreement with experimental data can be established when the ordinary Maxwell model restructured with fractional derivatives. Lei et al. [Lei, Liang and Xiao (2018)] demonstrated the development of two parallel fractional Maxwell's fluid (FMF) models to discuss the thermochemical trend of amorphous thermoplastics, viscous flow, and generate solutions for complex modulus and stress relaxation modulus.

Nearly, all the polymeric materials possess a viscoelastic trend which is difficult to interpret using conventional derivatives. Lin et al. [Liu and Liu (2018)] investigated the boundary layer flow (BLF) of FMF by introducing some suitable variables which enabled the conversion of the irregular boundaries of the stretching sheet to the regular one. The fractional governing equations were solved numerically using L1-scheme. Zhang et al. [Zhang, Shen, Liu et al. (2019)] studied the influence of thermophoresis, Brownian motion, diffusive heat transfer, and mass concentration in the flow of FMF near a moving plate. The numerical results were developed using L1-scheme and shifted the Grünwald formula with the introduction of novel dimensionless variables. Anwar et al. [Anwar and Rasheed (2018)] communicated the influence of Microscopic description of Joule heating, electric field, and MHD in nonlinear viscoelastic flow using fractional Cattaneo-Maxwell model. It was explored that fractional Cattaneo-Maxwell model is fit to control the temperature and concentration in resistive flow, oscillations, and relaxation processes that lead to memory formalism and delay of diffusion and thermal flux. Sadiq et al. [Sadiq, Imran, Fetecau et al. (2019)] analyzed the rotational flow of FMF in a cylindrical tube with a static couple shear stress via the joint Laplace and Henkel transforms. Yang et al. [Yang, Qi and Jiang (2018)] numerically studied the flow of FMF in a rectangular microchannel with the electroosmotic effect. Some recent developments which show the

supremacy of the FMF model over the Maxwell model with convectional derivative can be seen in Bai et al. [Bai, Huo, Zhang et al. (2019); Chen, Yang, Zhang et al. (2019); Raza and Asad Ullah (2020)] and the references therein.

The study of electrically conducting viscoelastic fluid flow with magnetohydrodynamic (MHD) effect in a porous media is very important because of its industrial, agricultural, astrophysical and geothermal applications [Ali, Saqib, Khan et al. (2016); Ali, Saqib, Khan et al. (2017a)]. It is established that when fluids comprising residues of minerals, flow under the action of the magnetic field generates Lorentz force. This force alters the physical characteristics of solid particles in the fluids, inhibiting the motion of heat exchanger along with the removal of viz if formed. The MHD filters and Meckling's MHD units are used in the heat exchanger to control scaling. The Mackling's MHD units are demonstrated to be advantageous for irrigation to improve the production of crops. These days, the idea of convection heat transfer in a porous media has been enormously applied in MHD flows to control the boundary layer of the fluids in close proximity to the boundaries, enhanced recovery of gas and petroleum, geothermal energy extraction, metallurgy, stirring of molten metal and improved the performance of various engineering tools such as controlled thermonuclear reactors, MHD flow-meters, MHD accelerators, MHD pumps, and MHD energy generators. Keeping in observation the significance and importance of MHD [Khan, Hussanan, Saqib et al. (2019)], MHD flow in a porous medium is considered.

These days (this year and the last few years) in the literature, several articles in applied mathematics, fluid dynamics, and thermal engineering are published using fractional derivatives (Caputo; Caputo-Fabrizio and Atangana Baleanu derivatives) studied fluid motion, heat transfer, mass transfer for different geometries. The idea of these fractional derivatives is also applied to several problems of viscoelastic fluids [Ali, Saqib, Khan et al. (2017b); Saqib, Ali, Khan et al. (2018); Saqib, Khan and Shafie (2018, 2019)]. However, most of these problems (fluid problems), were studied analytically using different integral transform techniques, as most of these problems are linear. The idea of the above fractional derivatives is rarely applied to fluid problems governed by nonlinear partial differential equations. Most importantly, the fractional models are developed by artificial replacement of the classical derivatives with fractional derivatives that are solved for fractional results. In the present article, (i) the unsteady nonlinear non-Newtonian fluid problem (Cattaneo-Friedrich Maxwell (CFM) model) is considered and (ii) the fractional model is developed from the initial fractional constitutive equations to the fractional governing equations, more exactly, the artificial replacement of the classical derivatives with fractional derivatives are not done but in details, the fractional problem is modeled from the fractional constitutive equations. More exactly, the flow of FMF over an inclined plate with variable velocity and temperature using the Cattaneo-Friedrich Maxwell model is studied.

## **2 Mathematical formulation**

The incompressible 2D MHD flow of FMF together with variable radiative heat transfer over an inclined moving plate, parallel to the  $x$ -axis, has been considered using Cattaneo and Friedrich constitutive equations for heat flux and shear stress respectively. An incline

magnetic field is applied to the  $y$ -direction whereas the fluid velocity is assumed in the  $x$ -direction. The velocity field is chosen of the following form

$$\mathbf{V}=(u(x,y,t),v(x,y,t),0) \quad (1)$$

Here the  $v$  component of the velocity vector in the  $y$ -direction is neglected in the energy and momentum equations because the fluid flow is assumed to be in the  $x$ -direction (horizontal direction). Taking into account the Boussinesq approximation, the momentum equation of the proposed model is written as Shafie et al. [Shafie, Saqib, Khan et al. (2019)]

$$\frac{\partial u}{\partial x} + \frac{\partial v}{\partial y} = 0 \quad (2)$$

$$\rho \left( \frac{\partial u}{\partial t} + u \frac{\partial u}{\partial x} + v \frac{\partial u}{\partial y} \right) = \frac{\partial \tau_{xy}}{\partial y} - \sigma B_0^2 \sin \phi u + R_x + \rho g \beta_T (T - T_\infty) \cos \psi \quad (3)$$

where  $\rho$  is density,  $u$  is  $x$ -component of velocity,  $v$  is  $y$ -component of velocity,  $\mu$  is dynamic viscosity,  $\sigma$  is electrical conductivity,  $B_0$  is the magnetic field in the  $y$ -direction,  $R_x$  is the Darcy's resistance,  $g$  is the gravitational acceleration and  $\beta_T$  is volumetric thermal expansion. The fractional constitutive equation of Maxwell fluid proposed by Friedrich [Friedrich (1991)] is given by

$$\tau_{xy} + \lambda_1^\alpha D_t^\alpha \tau_{xy} = \mu \frac{\partial u}{\partial y}, \quad (4)$$

which yield to

$$(1 + \lambda_1^\alpha D_t^\alpha) \tau_{xy} = \mu \frac{\partial u}{\partial y}, \quad (5)$$

where  $\lambda_1$  is relaxation time and  $D_t^\alpha(\dots)$  is Caputo time-fractional derivative with fractional order  $\alpha$ ;  $0 < \alpha < 1$  which can be expressed as [Ali, Sheikh, Khan et al. (2017)]

$$D_t^\alpha f(t) = \frac{1}{\Gamma(n-\alpha)} \int_0^t (t-s)^{n-\alpha-1} \frac{\partial^n f(s)}{\partial s^n} ds, n-1 < \Re\{\alpha\} < n, n \in \mathbb{N}, \quad (6)$$

with  $\Gamma(\cdot)$  is Gamma function given by [Ali, Sheikh, Khan et al. (2017)]

$$\Gamma(z) = \int_{\mathbb{R}} \eta^{z-1} e^{-\eta} d\eta, z \in \mathbb{C}, \Re\{z\} > 0. \quad (7)$$

Eliminating  $\tau_{xy}$  from Eqs. (3) and (5) yield to

$$\rho(1 + \lambda_1^\alpha D_t^\alpha) \left( \frac{\partial u}{\partial t} + u \frac{\partial u}{\partial x} + v \frac{\partial u}{\partial y} \right) = \mu \frac{\partial^2 u}{\partial y^2} - (1 + \lambda_1^\alpha D_t^\alpha) \sigma B_0^2 \sin \phi, \quad (8)$$

$$+ (1 + \lambda_1^\alpha D_t^\alpha) R_x + (1 + \lambda_1^\alpha D_t^\alpha) \rho g \beta_T (T - T_\infty) \cos \psi.$$

where  $(1 + \lambda_1^\alpha D_t^\alpha) R_x = -\mu\phi / k_p u$  satisfy the Darcy's in Eq. (8). The plate temperature is assumed to be  $T_w$  and on the surface of the plate, it is supposed to be  $T_\infty$  (the room temperature). The radiative temperature gradient is given by

$$\rho C_p \left( \frac{\partial T}{\partial t} + u \frac{\partial T}{\partial x} + v \frac{\partial T}{\partial y} \right) = -\nabla \cdot \mathbf{q}, \quad (9)$$

where  $C_p$  is the heat capacitance, and  $\mathbf{q}$  is the heat flux. As the heat flux is assumed in a vertical direction so, Eq. (9) takes the following form

$$\rho C_p \left( \frac{\partial T}{\partial t} + u \frac{\partial T}{\partial x} + v \frac{\partial T}{\partial y} \right) = -\frac{\partial \mathbf{q}}{\partial y}. \quad (10)$$

The heat flux  $\mathbf{q}$  in terms of the fractional derivative is generalized by Cattaneo [Cattaneo (1958)] using Fourier's law as

$$(1 + \lambda_2^\beta D_t^\beta) \mathbf{q} = -k \frac{\partial T}{\partial y}. \quad (11)$$

Eliminating  $\mathbf{q}$  from Eqs. (10) and (11) yield to

$$\rho C_p \left( \frac{\partial T}{\partial t} + u \frac{\partial T}{\partial x} + v \frac{\partial T}{\partial y} + \lambda_2^\beta D_t^{\beta+1} T \right) = k \frac{\partial^2 T}{\partial y^2} + \lambda_2^\beta D_t^\beta \left( u \frac{\partial T}{\partial x} \right) + \lambda_2^\beta D_t^\beta \left( v \frac{\partial T}{\partial y} \right). \quad (12)$$

Lastly, Eqs. (2), (8) and (12) Govern the proposed problem in terms of the fractional derivative as

$$\frac{\partial u}{\partial x} + \frac{\partial v}{\partial y} = 0 \quad (13)$$

subject to the following appropriate physical initial and boundary conditions

$$\rho \left( \frac{\partial u}{\partial t} + u \frac{\partial u}{\partial x} + v \frac{\partial u}{\partial y} + \lambda_1^\alpha D_t^{\alpha+1} u + \lambda_1^\alpha D_t^\alpha \left( u \frac{\partial u}{\partial x} \right) + \lambda_1^\alpha D_t^\alpha \left( v \frac{\partial u}{\partial y} \right) \right) = \mu \frac{\partial^2 u}{\partial y^2} - \lambda_1^\alpha D_t^\alpha \left( \sigma B_0^2 \sin \phi + \frac{\mu}{k_p} \right) u - \left( \sigma B_0^2 \sin \phi + \frac{\mu}{k_p} \right) u + \lambda_1^\alpha D_t^\alpha g \beta_T (T - T_\infty) \cos \psi, \quad (1)$$

$$\rho C_p \left( \frac{\partial T}{\partial t} + u \frac{\partial T}{\partial x} + v \frac{\partial T}{\partial y} + \lambda_2^\beta D_t^{\beta+1} T + \lambda_2^\beta D_t^\beta \left( u \frac{\partial T}{\partial x} \right) + \lambda_2^\beta D_t^\beta \left( v \frac{\partial T}{\partial y} \right) \right) = k \frac{\partial^2 T}{\partial y^2}, \quad (2)$$

subject to the following appropriate physical initial and boundary conditions

$$\left. \begin{aligned} u = 0, v = 0, T = T_\infty & \quad \text{at } t \leq 0, \\ u = 0, v = 0, T = T_\infty & \quad \text{at } x = 0, t > 0, \\ u = 0, T = T_w & \quad \text{at } y = 0, t > 0, \\ u \rightarrow 0, T \rightarrow T_\infty & \quad \text{at } y \rightarrow \infty, t > 0. \end{aligned} \right\} \quad (16)$$

The following non-similarity variables are introduced

$$t^* = \frac{t}{d^2}, y^* = \frac{y}{d}, x^* = \frac{x}{U_0 d^2}, u^* = \frac{u}{U_0}, v^* = \frac{dv}{U_0}, \quad (17)$$

$$\lambda_1^* = \lambda_1 \left( \frac{\nu}{d^2} \right), \lambda_2^* = \lambda_2 \left( \frac{\nu}{d^2} \right), \Phi = \frac{T - T_\infty}{T_w - T_\infty}$$

into Eqs. (13)-(16) and propping \* symbol for simplicity yield to

$$\frac{\partial u}{\partial x} + \frac{\partial v}{\partial y} = 0, \quad (18)$$

$$\frac{\partial u}{\partial t} + u \frac{\partial u}{\partial x} + v \frac{\partial u}{\partial y} + \lambda_1^\alpha D_t^{\alpha+1} u + \lambda_1^\alpha D_t^\alpha \left( u \frac{\partial u}{\partial x} \right) + \lambda_1^\alpha D_t^\alpha \left( v \frac{\partial u}{\partial y} \right) = \frac{\partial^2 u}{\partial y^2} - M \sin \phi \lambda_1^\alpha D_t^\alpha u - M \sin \phi u - \frac{u}{K} + \lambda_1^\alpha D_t^\alpha \Phi Gr \cos \psi + \Phi Gr \cos \psi \quad (19)$$

$$\frac{\partial \Phi}{\partial t} + u \frac{\partial \Phi}{\partial x} + v \frac{\partial \Phi}{\partial y} + \lambda_2^\beta D_t^{\beta+1} \Phi + \lambda_2^\beta D_t^\beta \left( u \frac{\partial \Phi}{\partial x} \right) + \lambda_2^\beta D_t^\beta \left( v \frac{\partial \Phi}{\partial y} \right) = \frac{1}{Pr} \frac{\partial^2 \Phi}{\partial y^2}, \quad (20)$$

$$\left. \begin{aligned} u = 0, v = 0, \Phi = 0 & \quad \text{at } t \leq 0, \\ u = 0, v = 0, \Phi = 0 & \quad \text{at } x = 0, t > 0, \\ u = 0, \Phi = 1 & \quad \text{at } y = 0, t > 0, \\ u \rightarrow 0, T \rightarrow 0 & \quad \text{at } y \rightarrow \infty, t > 0. \end{aligned} \right\} \quad (21)$$

where

$$M = \frac{d^2 \sigma B_0^2}{\mu}, K = \frac{k_p}{\phi d^2}, Gr = \frac{d^2 g \beta_T (T_w - T_\infty)}{\nu U_0}, Pr = \frac{\mu C_p}{k}$$

is the magnetic parameter, permeability of the porous medium, thermal Grashof number, radiation parameter, and Prandtl number respectively.

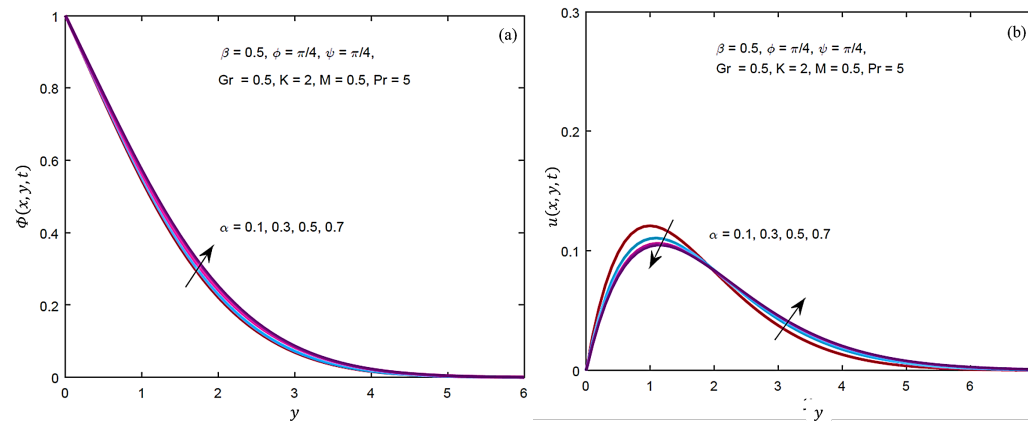


**Figure 1:** Consequence of  $\alpha$  on velocity and temperature filed when  $\beta = 0.5$ ,  $\phi = \pi / 4$ ,  $\psi = \pi / 4$ ,  $Gr = 0.2$ ,  $K = 2$ ,  $M = 0.5$  and  $Pr = 5$

### 3 Numerical scheme

This section concisely discusses the numerical method utilized for the solutions of Eqs. (19)-(21). The FDM together with L1-scheme [Liu, Zhuang, Anh et al. (2007)] for the discretization of fractional derivative appears in the model, is used for the numerical solutions. The numerical solutions are explicitly and semi-implicitly analyzed with two sorts of discretization. It is noticed that this method depends on the correct choice of fractional parameters  $\alpha$ ,  $\beta$  and choices as L2 and L2C are discussed in the literature for the discretization of fractional derivatives [Lynch, Carreras, del-Castillo-Negrete et al. (2003)]. It is indicated in the literature that the selection of L2-scheme is suitable for fast convergence when  $\alpha > 1.5$ . However, L2C-scheme shows better results for  $\alpha < 1.5$ .

Liu et al. [Liu, Zhuang, Anh et al. (2007)] are the pioneer of L1-scheme. They indicated that L1-scheme for fractional terms involved and FDM for the non-linear convective part of the model. The L1-scheme is superior to the other two because it is independent of the discretization choice and values of the fractional parameter  $\alpha$ . In the open literature,

some substantial numerical results are obtained from various fractional models using this method see, [Cao, Zhao, Wang et al. (2016); Khan and Rasheed (2019)] and the references therein. The L1-scheme and finite difference methods are the best fit for the problem under consideration. The detailed discretization can be found in Khan et al. [Khan and Rasheed (2019)].

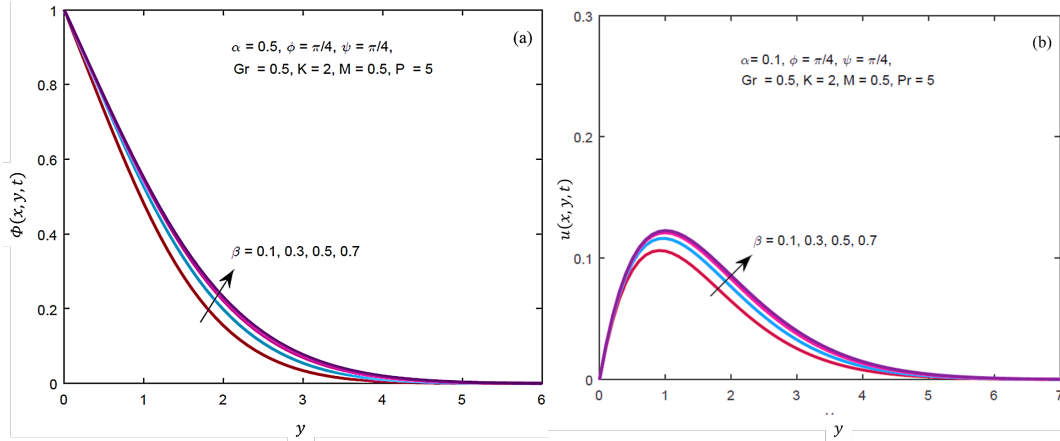


**Figure 2:** Consequence of  $\beta$  on velocity and temperature filed when  $\alpha = 0.5$ ,  $\phi = \pi / 4$ ,  $\psi = \pi / 4$ ,  $Gr = 0.2$ ,  $K = 2$ ,  $M = 0.5$  and  $Pr = 5$

#### 4 Result and discussion

This section presents the physical aspects of the numerical solutions obtained via FDM and the newly introduced L1 scheme. The numerical results are displayed in various graphs and the influence of fractional parameters  $\alpha, \beta$ , magnetic parameter  $M$ , angle of inclination of the magnetic field  $\phi$ , the permeability of the porous medium  $K$ , thermal Grashof number  $Gr$ , angle of inclination of the plate  $\psi$ , and Prandtl number  $Pr$  on the temperature and velocity profiles are studied. Finally, the three-dimensional view of the temperature and velocity profiles are portrayed.

Figs. 1(a) and 1(b) depict the effect of fractional parameter  $\alpha$  chosen for the momentum equation on temperature and velocity profiles. It is observed from Figs. 1(b) that the velocity profile shows a dual behavior. Near the plate, the velocity profile decreases with increasing values of  $\alpha$ ;  $0 < \alpha < 1$ . Though, away from the plate, it shows an identical trend as a temperature profile. Both the temperature and velocity profiles increase with increasing values of  $\alpha$ . This trend indicates that both the thermal and momentum boundary layers thickness increases with increasing values of  $\alpha$  which give rise to temperature and velocity profiles. Nevertheless, this trend cannot be generalized because it depends on the values of other involved parameters and change in the trend can be noticed for some other values of the involved parameter. The thickness in thermal and momentum boundary layers in the flow domain can be observed.

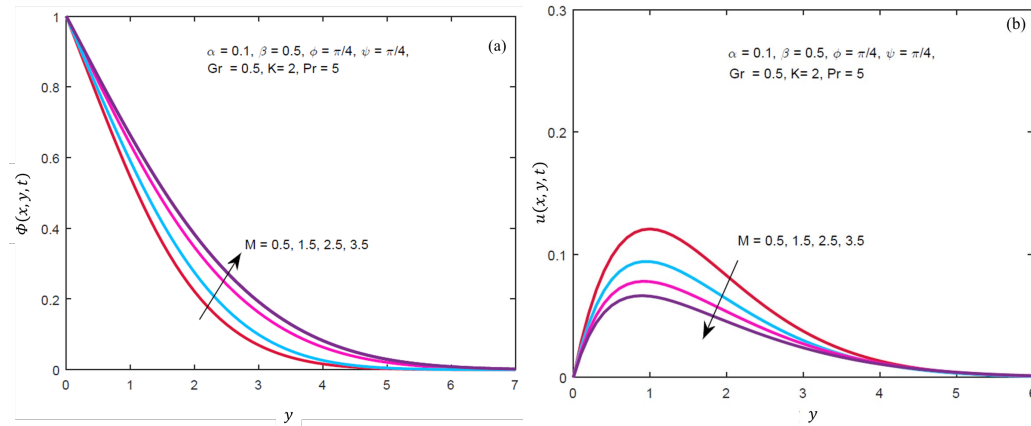


**Figure 3:** Consequence of  $M$  on velocity and temperature filed when  $\alpha = 0.5, \beta = 0.5, \phi = \pi / 4, \psi = \pi / 4, Gr = 0.2, K = 2,$  and  $Pr = 5$

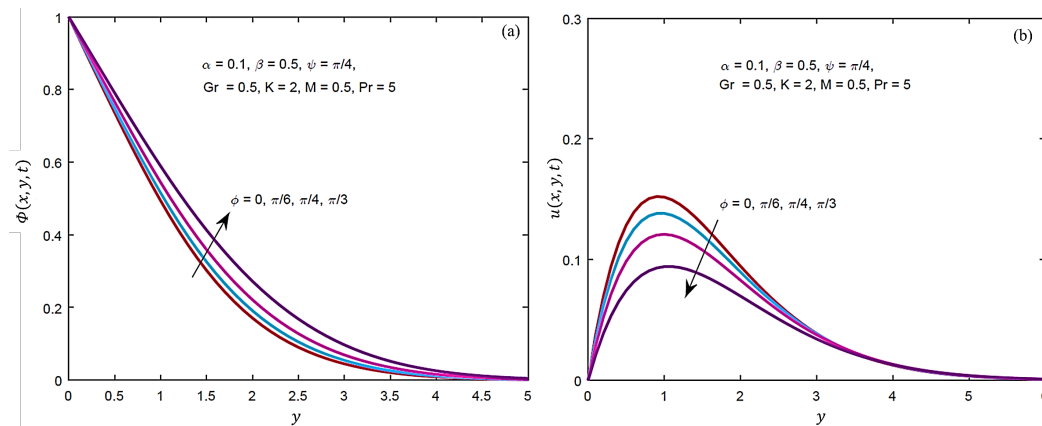


**Figure 4:** Consequence of  $\phi$  on velocity and temperature filed when  $\alpha = 0.5, \beta = 0.5, \psi = \pi / 4, Gr = 0.2, K = 2, M = 0.5$  and  $Pr = 5$

The effect of radiative heat transfer is with fraction Cattaneo heat flux of fractional parameter  $\beta$  is which similar as  $\alpha$ . In Figs. 2(a) and 2(b), a similar trend to  $\alpha$  on temperature and velocity profiles is observed. This is because the mixed convection takes place due to the temperature gradient. Increasing values of  $\beta$  offer a substantial increase in the temperature and velocity boundary layers.

The impact of the normal magnetic field on temperature and velocity profiles is presented in Figs. 3(a) and 3(b). These figures indicate that the effect of  $M$  on temperature and velocity profiles is the opposite. The velocity profile decreases with increasing values of  $M$  due to the increase in Lorentz forces which are similar to drag forces. Physically, when Lorentz forces increased it give rise to magnetic resistance, as a result, the velocity retarded. However, this trend is opposite in case of temperature profile since high resistance produces more heat due to high frictional force.

The influence of the angle of inclination  $\phi$  of the magnetic parameter  $M$  is depicted in Figs. 4(a) and 4(b) on temperature and velocity profiles. The case  $\phi = 0$  corresponds to the flow of FMF in the absence of a magnetic field. In this case, the velocity is high at a lower temperature because of the nonappearance of magnetic resistance. Although, the velocity decreases with increasing value of  $\phi$  and became a minimum when the magnetic field is normal for that reason the resistance strengthens at this stage. On the other hand, the temperature goes high due to high resistance. Figs. 5(a) and 5(b) present the consequence of permeability of porous medium  $K$  on the temperature and velocity profiles. The velocity increases with increasing values of  $K$ . Greater values of  $K$  corresponds to high permeability which reduces the friction of porous medium, as a result, the velocity increases. But the temperature profile shows a decreasing trend since with high permeability, the frictional force decreases which decrease in the temperature field.

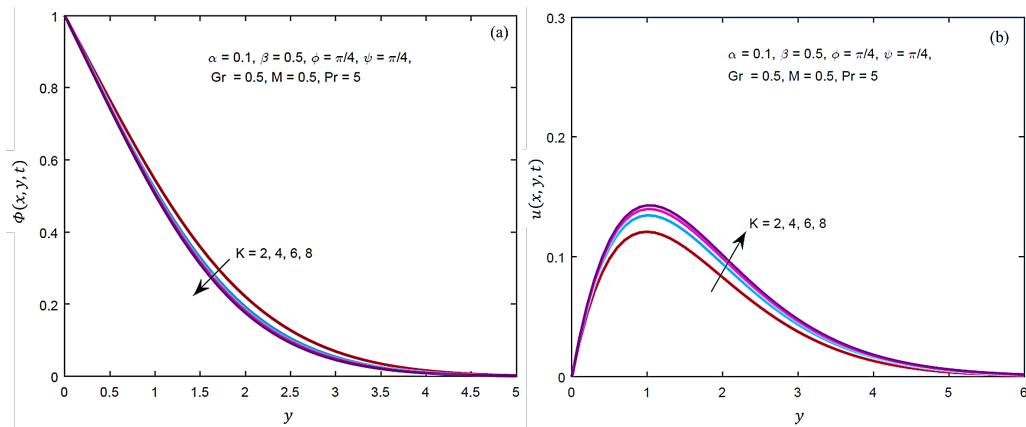


**Figure 5:** Consequence of  $K$  on velocity and temperature filed when  $\alpha = 0.5$ ,  $\beta = 0.5$ ,  $\phi = \pi / 4$ ,  $\psi = \pi / 4$ ,  $Gr = 0.2$ ,  $M = 0.5$  and  $Pr = 5$

Figs. 6(a) and 6(b) show variation in temperature and velocity profile for various values of  $Gr$ . The velocity of FMF increases with increasing values of values  $Gr$ . Physically, greater values of  $Gr$  giving rise to buoyancy force, for this reason, additional mixed convection occurs subsequently the velocity significantly increases. Nevertheless, this trend is the opposite of the temperature profile.

Figs. 7(a) and 7(b) are plotted to study the influence of the Prandtl number  $Pr$  on temperature and velocity profiles. Prandtl number is the ratio of viscous forces to the thermal conductivity. From the governing equation, it can be clearly seen that viscous forces are directly related to the velocity and temperature of FMF. When the Prandtl number increase it gives rise to viscous forces and falls in the thermal conductivity due to which both the temperature and velocity profile show a decreasing trend. In Figs. 8(a) and 8(b) and Figs. 9(a) and 9(b) are plotted to show the three-dimensional view of temperature and velocity and profiles which indicate excellent stability and convergence of the adopted numerical scheme

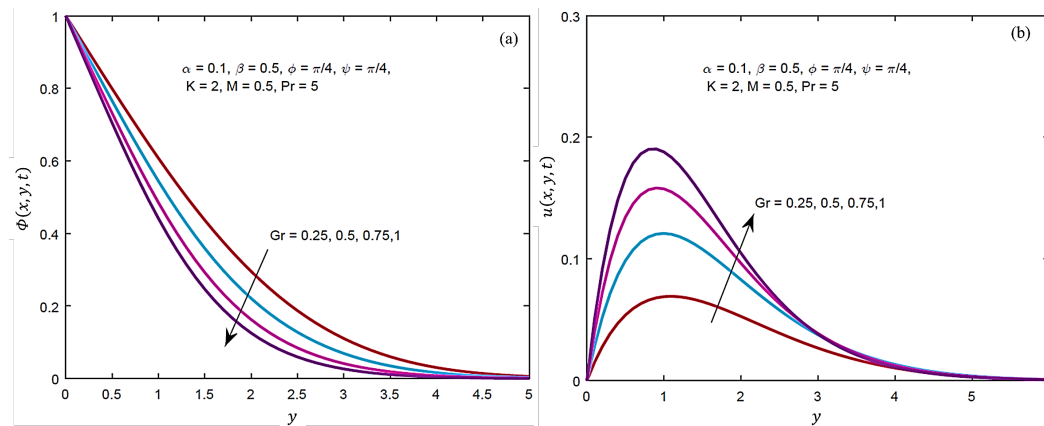


**Figure 6:** Consequence of  $Gr$  on velocity and temperature field when  $\alpha = 0.5$ ,  $\beta = 0.5$ ,  $\phi = \pi/4$ ,  $\psi = \pi/4$ ,  $K = 2$ ,  $M = 0.5$  and  $Pr = 5$

### 5 Concluding remarks

This manuscript presented the unsteady incompressible MHD flow of non-linear fractional Maxwell fluid over an inclined plate. The governing equations of the flow phenomena are modeled using Cattaneo-Friedrich fractional approach. An inclined magnetic field is applied to the plate with variable temperature and velocity boundary conditions. The numerical solutions are obtained using FDM and L1-schemes. The obtained results are plotted and studied physically. The two fractional parameters  $\alpha$  and  $\beta$  are introduced in momentum and energy equations respectively. The major findings of this study are as follow

1. It studied that both the fractional parameters behave in a similar manner. However, near the plate, the behavior of  $\alpha$  on velocity profiles is opposite to that of the temperature profile. But this trend is not general. It depends on the other parameters involved in the model.
2. It is noticed the normal magnetic resistance is high which reduces the velocity but increases the temperature due to frictional force.
3. The thermal Grashof number increases the velocity due to the occurrence of additional mixed convection.
4. Prandtl number decreases the velocity and temperature profiles because of the fall in thermal conductivity and the strengthen of viscous forces.
5. Finally, the three-dimensional view is observed that indicates that the chosen numerical scheme is stable and shows an excellent convergence.

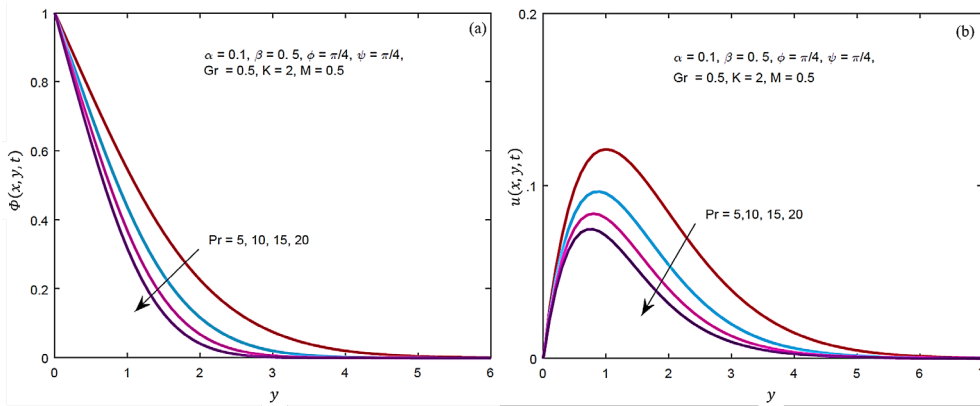


**Figure 7:** Consequence of Pr on velocity and temperature filed when  $\alpha = 0.5$ ,  $\beta = 0.5$ ,  $\phi = \pi / 4$ ,  $\psi = \pi / 4$ ,  $Gr = 0.2$ , and  $M = 0.5$

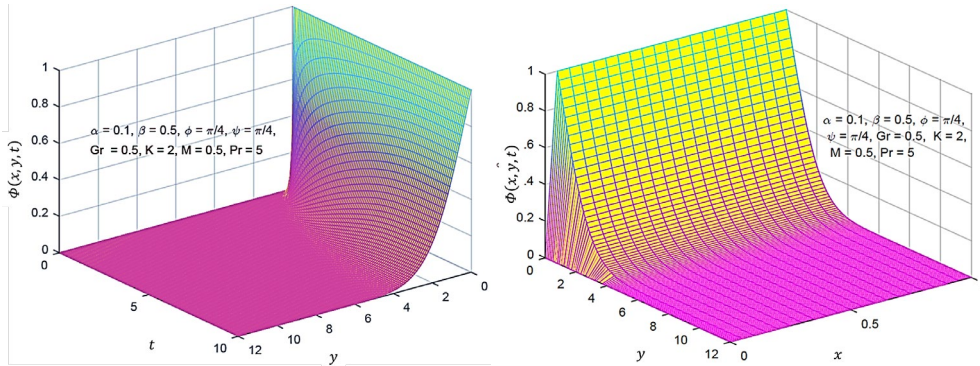


**Figure 8:** Three-dimensional temperature filed when  $\alpha = 0.5$ ,  $\beta = 0.5$ ,  $\phi = \pi / 4$ ,  $\psi = \pi / 4$ ,  $Gr = 0.2$ ,  $M = 0.5$  and  $Pr = 5$

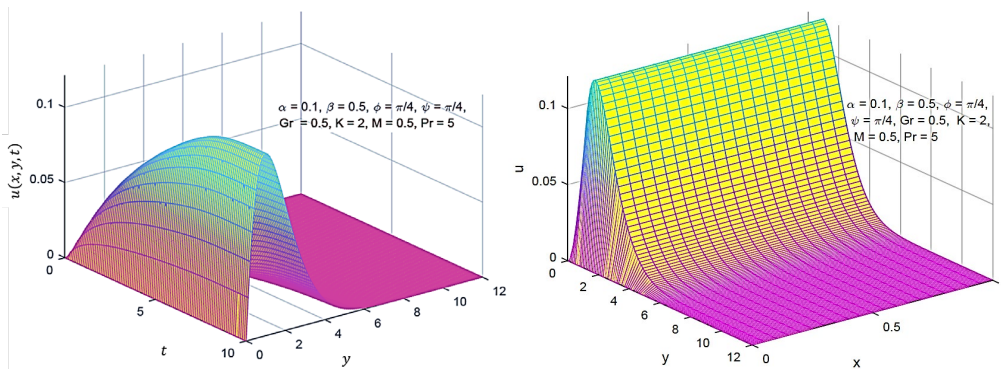


**Figure 9:** Three-dimensional velocity filed when  $\alpha = 0.5$ ,  $\beta = 0.5$ ,  $\phi = \pi / 4$ ,  $\psi = \pi / 4$ ,  $Gr = 0.2$ ,  $M = 0.5$  and  $Pr = 5$

**Funding Statement:** The authors would like to acknowledge Ministry of Education (MOE) and Research Management Centre-UTM, Universiti Teknologi Malaysia (UTM) for financial support through vote numbers 5F004, 5F278, 07G70, 07G72, 07G76, 07G77 and 08G33 for this research.

**Conflicts of Interest:** The authors declare that they have no conflicts of interest to report regarding the present study.

## References

- Ali, F.; Saqib, M.; Khan, I.; Sheikh, N. A.** (2016): Application of Caputo-Fabrizio derivatives to MHD free convection flow of generalized Walters'-B fluid model. *The European Physical Journal Plus*, vol. 131, no. 10, pp. 1-10.
- Ali, F.; Saqib, M.; Khan, I.; Sheikh, N. A.; Jan, S. A. A.** (2017a): Exact analysis of MHD flow of a Walters'-B fluid over an isothermal oscillating plate embedded in a porous medium. *The European Physical Journal Plus*, vol. 132, no. 2, pp. 1-14.
- Ali, F.; Saqib, M.; Khan, I.; Sheikh, N. A.; Jan, S. A. A.** (2017b): Exact analysis of MHD flow of a Walters'-B fluid over an isothermal oscillating plate embedded in a porous medium. *The European Physical Journal Plus*, vol. 132, no. 2, pp. 1-13.
- Ali, F.; Sheikh, N. A.; Khan, I.; Saqib, M.** (2017): Magnetic field effect on blood flow of Casson fluid in axisymmetric cylindrical tube: A fractional model. *Journal of Magnetism and Magnetic Materials*, vol. 423, no., pp. 327-336.
- Anwar, M. S.; Rasheed, A.** (2018): Joule heating in magnetic resistive flow with fractional Cattaneo–Maxwell model. *Journal of the Brazilian Society of Mechanical Sciences and Engineering*, vol. 40, no. 10, pp. 1-13.
- Bai, Y.; Huo, L.; Zhang, Y.; Jiang, Y.** (2019): Flow, heat and mass transfer of three-dimensional fractional Maxwell fluid over a bidirectional stretching plate with fractional Fourier's law and fractional Fick's law. *Computers & Mathematics with Applications*, vol. 78, no. 8, pp. 2871-2846.
- Cao, Z.; Zhao, J.; Wang, Z.; Liu, F.; Zheng, L.** (2016): MHD flow and heat transfer of fractional Maxwell viscoelastic nanofluid over a moving plate. *Journal of Molecular Liquids*, vol. 222, pp. 1121-1127.
- Cattaneo, C.** (1958): Sur une forme de l'équation de la chaleur éliminant la paradoxe d'une propagation instantanée. *Comptes Rendus*, vol. 247, pp. 431-433.
- Chen, X.; Yang, W.; Zhang, X.; Liu, F.** (2019): Unsteady boundary layer flow of viscoelastic MHD fluid with a double fractional Maxwell model. *Applied Mathematics Letters*, vol. 95, pp. 143-149.
- Friedrich, C.** (1991): Relaxation and retardation functions of the Maxwell model with fractional derivatives. *Rheologica Acta*, vol. 30, no. 2, pp. 151-158.
- Haque, E. U.; Awan, A. U.; Raza, N.; Abdullah, M.; Chaudhry, M. A.** (2018): A computational approach for the unsteady flow of Maxwell fluid with Caputo fractional derivatives. *Alexandria Engineering Journal*, vol. 57, no. 4, pp. 2601-2608.

- Khan, A. Q.; Rasheed, A.** (2019): Mixed convection magnetohydrodynamics flow of a nanofluid with heat transfer: a numerical study. *Mathematical Problems in Engineering*, vol. 2019, pp. 1-14.
- Khan, I.; Hussanan, A.; Saqib, M.; Shafie, S.** (2019): Convective heat transfer in drilling nanofluid with clay nanoparticles: applications in water cleaning process. *Bionanoscience*, vol. 9, no. 2, pp. 453-460.
- Khan, I.; Saqib, M.; Ali, F.** (2018): Application of the modern trend of fractional differentiation to the MHD flow of a generalized Casson fluid in a microchannel: Modelling and solution. *The European Physical Journal Plus*, vol. 133, no. 7, pp. 1-10.
- Lei, D.; Liang, Y.; Xiao, R.** (2018): A fractional model with parallel fractional Maxwell elements for amorphous thermoplastics. *Physica A: Statistical Mechanics and its Applications*, vol. 490, pp. 465-475.
- Liu, F.; Zhuang, P.; Anh, V.; Turner, I.; Burrage, K.** (2007): Stability and convergence of the difference methods for the space-time fractional advection-diffusion equation. *Applied Mathematics and Computation*, vol. 191, no. 1, pp. 12-20.
- Liu, L.; Liu, F.** (2018): Boundary layer flow of fractional Maxwell fluid over a stretching sheet with variable thickness. *Applied Mathematics Letters*, vol. 79, pp. 92-99.
- Lynch, V. E.; Carreras, B. A.; del-Castillo-Negrete, D.; Ferreira-Mejias, K.; Hicks, H.** (2003): Numerical methods for the solution of partial differential equations of fractional order. *Journal of Computational Physics*, vol. 192, no. 2, pp. 406-421.
- Makris, N.; Constantinou, M.** (1991): Fractional-derivative Maxwell model for viscous dampers. *Journal of Structural Engineering*, vol. 117, no. 9, pp. 2708-2724.
- Makris, N.; Dargush, G.; Constantinou, M.** (1993): Dynamic analysis of generalized viscoelastic fluids. *Journal of Engineering Mechanics*, vol. 119, no. 8, pp. 1663-1679.
- Raza, N.; Asad Ullah, M.** (2020): A comparative study of heat transfer analysis of fractional Maxwell fluid by using Caputo and Caputo-Fabrizio derivatives. *Canadian Journal of Physics*, vol. 98, no. 1, pp. 89-101.
- Sadiq, N.; Imran, M.; Fetecau, C.; Ahmed, N.** (2019): Rotational motion of fractional Maxwell fluids in a circular duct due to a time-dependent couple. *Boundary Value Problems*, vol. 2019, no. 1, pp. 1-11.
- Saqib, M.; Ali, F.; Khan, I.; Sheikh, N. A.; Jan, S. A. A.** (2018): Exact solutions for free convection flow of generalized Jeffrey fluid: a Caputo-Fabrizio fractional model. *Alexandria Engineering Journal*, vol. 57, no. 3, pp. 1849-1858.
- Saqib, M.; Khan, I.; Shafie, S.** (2018): Natural convection channel flow of CMC-based CNTs nanofluid. *The European Physical Journal Plus*, vol. 133, no. 12, pp. 1-16.
- Saqib, M.; Khan, I.; Shafie, S.** (2019): Shape effect in magnetohydrodynamic free convection flow of sodium alginate-ferrimagnetic nanofluid. *Journal of Thermal Science and Engineering Applications*, vol. 11, no. 4, pp. 1-8.
- Saqib, M.; Shafie, S.; Khan, I.; Chu, Y. M.; Nisar, K. S.** (2020): Symmetric MHD channel flow of nonlocal fractional model of BTF containing hybrid nanoparticles. *Symmetry*, vol. 12, no. 4, pp. 1-19.

**Shafie, S.; Saqib, M.; Khan, I.; Qushairi, A.** (2019). Mixed convection flow of Brinkman type hybrid nanofluid based on Atangana-Baleanu fractional model. *Proceedings of the 2019 Journal of Physics: Conference Series*, 1-10.

**Sheikh, N. A.; Ali, F.; Saqib, M.; Khan, I.; Jan, S. A. A.** (2017): A comparative study of Atangana-Baleanu and Caputo-Fabrizio fractional derivatives to the convective flow of a generalized Casson fluid. *The European Physical Journal Plus*, vol. 132, no. 1, pp. 1-14.

**Yang, X.; Qi, H.; Jiang, X.** (2018): Numerical analysis for electroosmotic flow of fractional Maxwell fluids. *Applied Mathematics Letters*, vol. 78, pp. 1-8.

**Zhang, M.; Shen, M.; Liu, F.; Zhang, H.** (2019): A new time and spatial fractional heat conduction model for Maxwell nanofluid in porous medium. *Computers & Mathematics with Applications*, vol. 78, no. 5, pp. 1621-1636.